

# Numerical investigations of scaling at the Anderson transition

Rudolf A Römer and Michael Schreiber

## 1 Introduction

At low temperature  $T$ , a significant difference between the behavior of crystals on the one hand and disordered solids on the other is seen: sufficiently strong disorder can give rise to a transition of the transport properties from conducting behavior with finite resistance  $R$  to insulating behavior with  $R = \infty$  as  $T \rightarrow 0$  as was pointed out by Anderson in 1958 [1]. This phenomenon is called the disorder-driven metal-insulator transition (MIT) [2, 3, 4] and it is characteristic to non-crystalline solids. The mechanism underlying this MIT was attributed by Anderson not to be due to a finite gap in the energy spectrum which is responsible for an MIT in band gap or Mott insulators [5]. Rather, he argued that the disorder will lead to interference of the electronic wave function  $\psi(x)$  with itself such that it is no longer extended over the whole solid but is instead confined to a small part of the solid. This *localization* effect excludes the possibility of diffusion at  $T = 0$  and thus the system is an insulator.

A highly successful theoretical approach to this disorder-induced MIT was put forward in 1979 by Abrahams *et al.* [6]. This “scaling hypothesis of localization” details the existence of an MIT for non-interacting electrons in three-dimensional (3D) disordered systems at zero magnetic field  $B$  and in the absence of spin-orbit coupling. The starting point for the approach is the realization that the sample-size ( $L^d$ ) dependence of the (extensive) conductance

$$G = \sigma L^{d-2} = g \frac{e^2}{h} \quad (1)$$

should be investigated [3] with  $\sigma$  denoting the conductivity,  $d$  the spatial dimension and  $g$  the dimensionless conductance. On the other hand, for strong disorder, the wave functions will be exponentially localized with localization length  $\lambda$  and thus the conductance in a finite system will be

$$g \sim \exp(-L/\lambda). \quad (2)$$

Defining the logarithmic derivative

$$\beta(g) = \frac{d \ln g}{d \ln L}, \quad (3)$$

we see from Eq. (1) that  $\beta < 0$  for  $d = 1$  and  $2$  and thus an increase in  $L$  will drive the system towards the insulator, there are no extended states and no MIT. However, the  $\beta$  curve for  $d = 3$  is positive for large  $g$  and negative for small  $g$  and an increase of  $L$  will drive the system either to metallic or to insulating behavior.

The scenario proposed by the scaling hypothesis is that of a continuous second-order quantum phase transition [4]. Then in the vicinity of the critical energy  $E_c$  the DC conductivity  $\sigma$  and the localization length  $\lambda$  should behave as

$$\sigma \propto (E - E_c)^s \text{ for } E \geq E_c, \quad (4)$$

$$\lambda \propto (E_c - E)^{-\nu} \text{ for } E \leq E_c. \quad (5)$$

with  $s = \nu(d - 2)$  due to further scaling relations [2]. Introducing a similarly defined dynamical exponent  $z$  for the temperature scaling as  $\sigma(T) \propto T^{1/z}$ , we can write the full finite-temperature scaling form as

$$\sigma(\mu, T) \propto [(\mu - E_c)/E_c]^s \mathcal{F} \left[ \frac{T}{[(\mu - E_c)/E_c]^{z\nu}} \right], \quad (6)$$

with  $\mu$  the chemical potential,  $\mathcal{F}$  the scaling function and  $z = d$  [7]. The special energy  $E_c$  is called the mobility edge [1] and separates localized states with  $|E| > E_c$  from extended states with  $|E| < E_c$ . States directly at the transition with  $E = E_c$  are called critical and will be examined later in much detail. In this way the disorder-driven MIT has been reformulated in terms of the theory of critical phenomena [2].

## 2 Experimental evidence in favor of scaling

Much work has subsequently supported these scaling arguments at  $B = 0$  experimentally, analytically and numerically [3]. The MIT can be observed by measuring the conductivity on the metallic side and the dielectric susceptibility on the insulating side of the transition [8]. For doped Si:P, many experiments have been performed following the original work of Paalanen and Thomas [9]. The one-parameter scaling hypothesis has been beautifully validated in these experiments by, e.g., constructing scaling curves for the conductivity [10]. The recent experiments in Si:P [11, 12, 13, 10] are concerned with the exact estimation of the critical exponent  $\nu$  as in Eq. (4). The current estimate is  $\nu \approx 1$ . The interest in the exact value of  $\nu$  arises since compensated semiconductors apparently have  $\nu \approx 1$  as do amorphous metals [14, 15, 8]. On the other hand, for uncompensated semiconductors one had previously found  $\nu \approx 0.5$  [9, 8]. The recent estimations of  $\nu \approx 1$  for *uncompensated* Si:P [10], based on a careful scaling analysis according to Eq. (6) and a consideration of various temperature regimes, may suggest at last a resolution of this “exponent puzzle” [16].

Other experiments in 3D have been performed, e.g., on Si:B [17,18]. Scaling according to Eq. (6) yields  $\nu = 1.6$ . The large value of  $\nu$  — as compared to the Si:P data — was attributed to the presence of interaction effects. An experimentally convenient way to construct very homogeneously disordered samples is the transmutation doping technique [19,20,21] which uses the homogeneous properties of neutron rays. Recent scaling results then suggest  $\nu = 1.6 \pm 0.2$  [22].

As the localization phenomenon in disordered solids is intrinsically due to the wave nature of the electrons, it can also be observed in other systems exhibiting wave motion [3]. Localization has been studied, e.g. for water waves [23] in shallow basins with random obstacles, for light waves [24,25,26] in the presence of a fine dust of semiconductor material, for microwaves [27,28] in microwave cavities with random scatterers, and also for surface plasmon polariton waves [29] on rough semiconducting surfaces.

### 3 Scaling and the Anderson model of localization

In order to describe a disordered system, let us consider the Anderson model of localization [1],

$$H = \sum_{j\alpha, k\beta} t_{j\alpha, k\beta} |j\alpha\rangle \langle k\beta| + \sum_{j\alpha} \epsilon_{j\alpha} |j\alpha\rangle \langle j\alpha|. \quad (7)$$

The off-diagonal matrix  $t_{j\alpha, k\beta}$  denotes the hopping integrals between the states  $\{\alpha\}$  at sites  $\{j\}$  with the states  $\{\beta\}$  at sites  $\{k\}$  and represents the discretization of the kinetic energy. For simplicity, one usually assumes that  $\alpha = \beta = 1$  such that there is only one state per site. Moreover, the hopping is usually restricted to nearest-neighbor sites. The disorder is incorporated into the diagonal matrix  $\epsilon_{j\alpha}$ , whose elements are random numbers usually taken from a uniform distribution  $[-W/2, W/2]$  with  $W$  parameterizing the strength of the disorder. Other distributions such as Gaussian and Lorentzian have also been investigated [30,34,31,32,33].

This model has been used extensively in conjunction with powerful numerical methods in order to study the localization problem [3]. MacKinnon and Kramer [35,36] have numerically verified the scaling hypothesis by showing that one can find the scaling behavior outlined in section 1. For 3D the corresponding scaling curves have two branches corresponding to the metallic and insulating phases, whereas in 1D and 2D only the insulating branch exists. Recent numerical results — some of which shall be presented in the coming sections — indicate that  $\nu = 1.58 \pm 0.02$  [37,38] which is in excellent agreement with the newer experiments reviewed above.

## 4 Numerical methods and finite-size scaling for disordered systems

The preferred numerical method for accurately computing localization lengths in disordered quantum systems is the transfer-matrix method (TMM) [39, 35, 36, 40]. The TMM is based on a recursive reformulation of the Schrödinger equation such that, e.g. in a 2D strip of width  $M$ , length  $N \gg M$  and uniform hopping  $t_{j,k} = 1$  between nearest neighbors only,

$$\psi_{n+1,m} = (E - \epsilon_{n,m})\psi_{n,m} - \psi_{n,m-1} - \psi_{n,m+1} - \psi_{n-1,m} \quad (8)$$

where  $\psi_{n,m}$  is the wave function at site  $(n, m)$ . Eq. (8) can be reformulated into a matrix equation as

$$\begin{pmatrix} \psi_{n+1} \\ \psi_n \end{pmatrix} = \begin{pmatrix} E - \epsilon_n - H_{\perp} & -1 \\ 1 & 0 \end{pmatrix} \begin{pmatrix} \psi_n \\ \psi_{n-1} \end{pmatrix} = T_n \begin{pmatrix} \psi_n \\ \psi_{n-1} \end{pmatrix}, \quad (9)$$

where  $\psi_n = (\psi_{n,1}, \dots, \psi_{n,M})^T$  denotes the wave function at all sites of the  $n$ th slice,  $\epsilon_n = \text{diag}(\epsilon_{n,1}, \dots, \epsilon_{n,M})$ , and  $H_{\perp}$  represents the hopping terms in the transverse direction. The evolution of the wave function is given by the product of the transfer matrices  $\tau_N = T_N T_{N-1} \dots T_2 T_1$ . Strong fluctuations, which increase exponentially with the system size, govern the evolution of the wave function and thus the behavior of the transmission coefficient through the sample [46, 42, 45, 43, 41, 44]. Only the logarithm of the transmission coefficient [35, 36, 39, 40, 42, 41] and the logarithm of the conductance [46, 47, 48] are statistically well-behaved self-averaging quantities. According to Oseledec's theorem [49] the eigenvalues  $\exp[\pm\gamma_i(M)]$  of  $\Gamma = \lim_{N \rightarrow \infty} (\tau_N^{\dagger} \tau_N)^{1/2N}$  exist and the smallest Lyapunov exponent  $\gamma_{\min} > 0$  determines the localization length  $\lambda(M) = 1/\gamma_{\min}$  at energy  $E$ . The accuracy of the  $\lambda$ 's is determined as outlined in Refs. [35, 36] from the variance of the changes of the exponents in the course of the iteration. Usually the method is performed with a complete and orthonormal set of initial vectors  $(\psi_1, \psi_0)^T$ . In order to preserve this orthogonality, the iterated vectors have to be reorthogonalized during the iteration process.

For small disorders, the  $\lambda(M)$  values are of the same order of magnitude as the strip width  $M$  and thus subject to finite-size modifications. In order to avoid simple extrapolation schemes, a finite-size scaling (FSS) technique had been developed in Refs. [35, 36, 40] based on real space renormalization arguments for systems with finite size  $M$  and intimately related to the original scaling approach [6, 50]. The connection to the experimentally perhaps more relevant finite-temperature scaling as in Eq. (6) is based on the idea that a finite system size  $M$  may be assumed to be equivalent to a measurement at finite temperature  $T$  since a finite temperature induces an effective length scale beyond which the electrons will scatter inelastically and thus lose the phase coherence necessary for quantum interference [2, 36]. Scaling the

$\lambda(M)/M$  data for various values of  $W$  onto a common scaling curve, i.e.,

$$\lambda(M)/M = f(\xi/M). \quad (10)$$

is the analogue of Eq. (6). One determines the FSS function  $f$  and the values of the scaling parameter  $\xi$  by a non-linear Levenberg-Marquardt fit [38], see also T. Ohtsuki's contribution in this volume. For diagonal disorder in 3D, this scaling hypothesis of localization has been shown to be valid with very high accuracy, and the  $\xi$  values of the extended (localized) branch are equal to the correlation (localization) length in the infinite system. A similar method based on the recursive Green's function technique is discussed by A. MacKinnon in this volume.

A number of more indirect numerical approaches to the MIT have been developed that either only require selected parts of the spectrum — so-called energy-level statistics (ELS) — or a few selected eigenvectors in the spectrum — so-called wave-function statistics (WFS) [51, 52, 53]. These methods are based on the connection of Anderson localization to random matrix theory (RMT) [54, 55].

The (inverse) participation number [56] represents another possibility to distinguish localized states [57], its scaling with the system size yields a characteristic fractal dimension [62, 58, 59, 63, 60, 64, 61]. A generalization to higher moments of the spatial distribution of the wave function leads to the multifractal analysis (MFA) [66, 65], where one computes a spectrum of exponents to describe scaling properties of the wave function [67, 73, 71, 72, 76, 74, 75, 66, 68, 69, 70]. For a given disorder, one can then read off from the system-size dependence whether the spectrum tends towards the metallic, insulating or truly critical behavior. At the MIT the singularity spectrum of the MFA is independent of the system size [76, 75, 77]. Thus we again have a means of studying the MIT. Note that WFS and MFA are not independent of each other, but one may be derived from the other [78]. The fractal characteristics of the eigenstates, i.e their scale invariance, can be beautifully visualized [79, 80] by displaying the curdling of the wave functions at the MIT.

## 5 Scaling for non-interacting, disordered systems

### 5.1 Early scaling results for the isotropic Anderson model

Following the seminal papers of MacKinnon and Kramer [35, 36] the TMM and FSS approach was used to determine the phase diagram of localization i.e. the MIT in the entire  $(E, W)$  plane for the isotropic Anderson model with diagonal box, Gaussian and Lorentzian disorders [34, 31, 32, 33, 81] as well as at the band center for a binary [82] and a triangular distribution [83]. In 2D, not only the usual square lattice, but also a triangular and honeycomb lattice was studied [84]. The derivation of the critical exponents in these early studies was, however, impeded by the relatively large error of 1 % of

the raw data and the limited cross section size of typically up to  $M^2 = 13^2$  sites [86, 85, 83, 84]. Much effort was needed to determine reliable values of  $\nu$  [85, 82].

We note that FSS has also been successfully employed for the analysis of ELS data and the derivation of critical exponents from the cumulative level-spacing distribution and Dyson-Metha statistics [87, 88].

The scaling of the participation number has further been investigated for the Anderson model on 2D and 3D quasiperiodic lattices, too [90, 89]. By means of FSS of the participation number, the MIT and the critical exponent could be computed [89].

The entire phase diagram of localization has also been established by MFA of the isotropic Anderson model with box, Gaussian and binary disorder [75], determining the parameter combinations of  $E$  and  $W$  for which the singularity spectrum is scale-invariant.

## 5.2 The Anderson model with anisotropic hopping

As shown in section 1, there is no MIT in 2D in the absence of many-body interactions, magnetic field and spin-orbit interactions. Furthermore, the  $2 + \epsilon$  expansion within the non-linear  $\sigma$  model [7] and numerical studies based on TMM data for bi-fractals [91] suggest that the critical exponent in  $2 + \epsilon$  dimensions changes continuously as  $\epsilon \rightarrow 0$  for  $\epsilon$  between 0 and 1. Thus one is led to ask the question whether a similarly continuous change does also happen, if we vary the hopping elements anisotropically (see C. Soukoulis in this volume). E.g., we decrease the hopping homogeneously in one or two directions yielding weakly coupled planes or chains. This then might model a transition from 3D to 2D or 1D, respectively.

We have investigated this problem using MFA [92, 88], TMM [93, 88] and ELS [94, 95, 88] together with FSS. We find that the critical disorder changes continuously with decreasing hopping strength  $t_a$  such that  $W_c \sim t_a^\alpha$ , where  $\alpha$  is close to  $\frac{1}{4}$  for planes and  $\frac{1}{2}$  for chains. Here  $a$  represents  $z$  for coupled planes and  $y$  and  $z$  for chains. In Fig. 1 we show examples of FSS in this model. Note that the small relative error 0.07% of the raw data as well as the large system cross sections up to  $M^2 = 46^2$  [94] (not shown here) for TMM make it possible — besides taking into account non-linear deviations from  $|1 - \frac{W}{W_c}|$  — to determine estimates for *irrelevant* scaling exponents [38]. The value of the critical exponent  $\nu$  is not affected by the anisotropy [96] and retains its usual value  $1.6 \pm 0.1$  as in 3D [37, 38]. Thus the 2D and 1D cases are reached only for  $t_a = 0$  and we observe the 3D MIT at any finite  $t_a$ .

The ELS and the singularity spectrum of the MFA at the MIT are independent of the system size and this size independence can be used to identify the MIT [97, 98, 87, 68, 69, 70, 99]. However, both ELS and MFA are influenced by the anisotropy and change considerably in comparison to the isotropic case. Also, the eigenfunctions are different from the isotropic case. Therefore ELS and the MFA singularity spectrum at the MIT are not universal, i.e.,

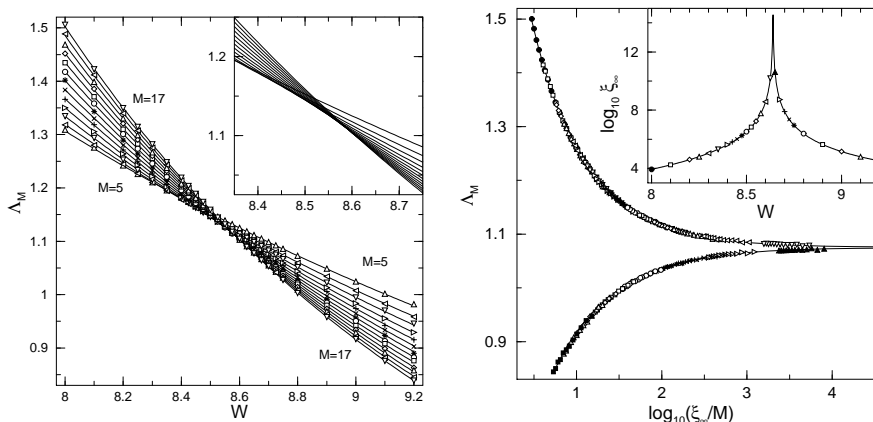


**Fig. 1.** Left: Reduced localization length for coupled planes with  $t_z = 0.1$  and  $M = 5, 6, \dots, 17$ . The lines are fits of the data according to [38] with  $n_r = 3$  and  $m_r = 2$ . In the inset we enlarge the central region without the data points to show the shift of the crossing point. Right: Scaling function and scaling parameter, shown in the inset, corresponding to the fit in the left panel. The symbols distinguish different  $W$  values of the scaled data points.

not independent of microscopic details of the system. This dependence on microscopic details is similar to the dependence on boundary conditions established recently for the ELS at the MIT [100, 101]. However, the critical exponent should, of course, be universal. As it turned out [94, 95], FSS can be applied successfully to various statistics of the spectrum, most accurately to the integrated  $\Sigma_2$  and  $\Delta_3$  statistics. In Fig. 2, we give scaling results for the integrated  $\Sigma_2$  statistics ( $\eta$ ) and its derivative, the so-called level compressibility  $\chi$ , both of which have been computed from spectral data with error 0.2 – 0.4%. The critical exponents  $\nu_\eta = 1.43 \pm 0.13$ ,  $\nu_\chi = 1.47 \pm 0.10$  derived from these data [95], although less accurate, are in agreement with the above-mentioned values.

### 5.3 The Anderson model with random hopping

Let us change the model (7) such that all nearest-neighbor  $t$  values can be chosen randomly [102] with, e.g.,  $t \in [c - w/2, c + w/2]$  with  $c$  and  $w$  denoting the center and width of the distribution. In this parameterization, the ordered tight-binding model is recovered in the limit  $c \rightarrow \infty$  after a suitable rescaling. The DOS has a peak at energy  $E = 0$  for any strength of hopping disorder — known in 1D as *Dyson singularity* [103] — and the localization length at  $E = 0$  diverges even in 1D [104].

We have studied the random hopping model in 2D [105, 106, 107] by TMM and by direct diagonalization of the Hamiltonian matrix and have shown that the singularity in the DOS still exists for bipartite square lattices where

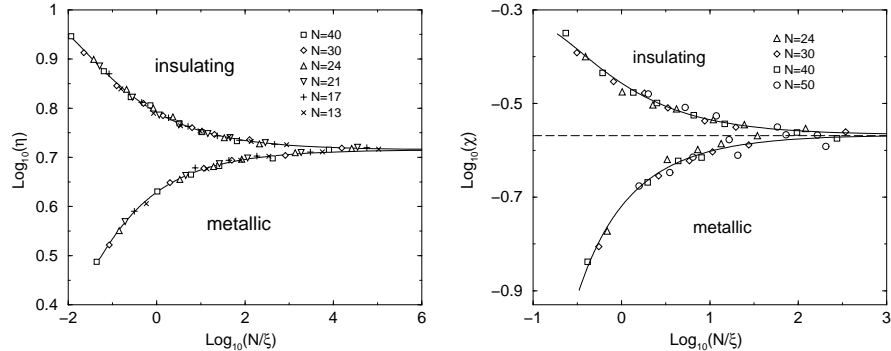


**Fig. 2.** Left: The one-parameter scaling dependence of  $\eta$  on  $\xi$  for different system sizes  $N$  and disorders  $W \in [6, 12]$ . Right: The one-parameter scaling dependence of  $\chi$ . The dashed line indicates the value  $\chi_c = 0.27$  at the MIT obtained from this fit.

the energy spectrum is strictly symmetric around  $E = 0$ . Furthermore, the localization length is also diverging at  $E = 0$  [108, 109, 110, 111], see also S. Evangelou's contribution in the volume.

For sufficiently large energies, it has been suggested [111] that the divergence of the localization length at the band center may be described by a power law, whereas it takes more complicated form below a certain crossover energy  $E^*$ . Our results at 0.1% error in the raw data for 2D suggest that the localization lengths exhibit power-law behaviour in a wide energy range with lower bound  $E_{\min} \approx 10^{-7}$  and non-universal exponents  $\nu \approx 0.25$  [112], see Fig. 3. For smaller energies we observe some deviations, however, there is also a possibility that this may be an effect of pronounced convergence problems which appear for strong hopping disorder.

In 3D, the hopping disorder alone is no longer sufficient to localize all states [102] as happens for (uniform) diagonal disorder at  $W_c = 16.5$ . Results of FSS for the 3D system at 0.1% error indicate that the critical exponent  $\nu$  is the same regardless whether we study the MIT as a function of  $E$  or as a function of additional diagonal disorder  $W$ . Taking into account irrelevant scaling terms, we find that  $\nu = 1.59 \pm 0.05$ . Thus the results are again in agreement with the usual 3D case and the scaling hypothesis [114, 113].

#### 5.4 Thermoelectric transport coefficients in the Anderson model

The conductivity  $\sigma$  is the quantity which is most often studied in transport measurements of disordered systems [17, 18, 9, 11, 12, 13, 115, 10]. However, other transport properties such as the thermopower  $S$ , the thermal conductivity  $K$  and the Lorenz number  $L_0$  have also been measured [116, 117, 118]. In Refs. [119, 120, 121], we have studied the behavior of  $S$ ,  $K$  and  $L_0$  by straightforwardly calculating the integrals in the linear response formulation



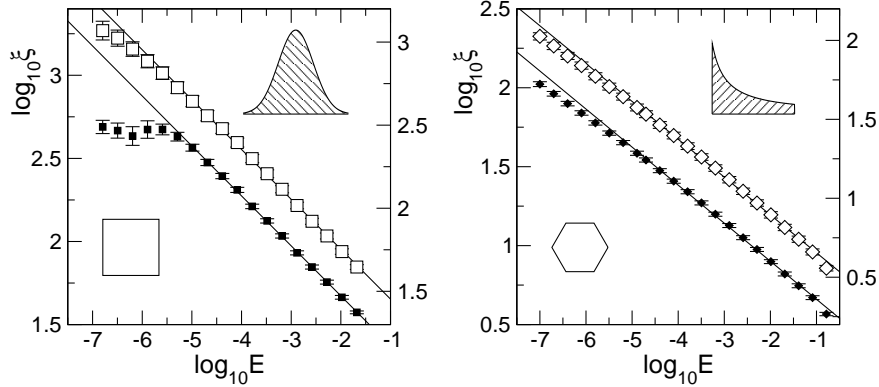


**Fig. 3.** Scaling parameter  $\xi$  vs. energy. Left panel: square lattice, Gaussian  $t$  distribution, right panel: honeycomb lattice, logarithmic  $t$  distribution; filled symbols: results for  $M = 50$ – $100$ , open symbols: results for  $M = 110$ – $160$  (Gaussian distribution) or  $M = 100$ – $150$  (logarithmic distribution).

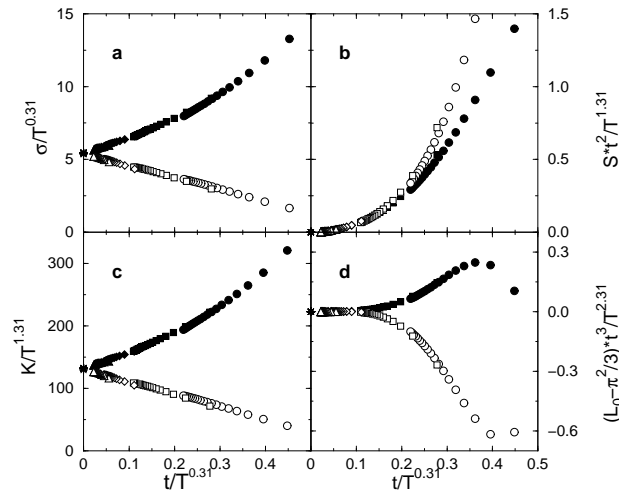


**Fig. 4.** Scaling of thermoelectric transport properties where  $t = |1 - E_F/E_c|$ . The different symbols denote the relative positions of various values of the Fermi energy  $E_F$  with respect to the mobility edge  $E_c$ .

of Chester-Greenwood-Kubo-Thellung [122, 123, 124]. The only additional ingredients in our study were an averaged DOS and (a) the assumption of  $\sigma(E)$  as in Eq. (4) [30, 75] or (b) an energy-dependent conductivity  $\sigma$  obtained experimentally. For (a), we can show that the previous analytical considerations [125, 126, 127] apply in limited regimes of validity. Thus  $S/T$  diverges as  $T \rightarrow 0$  when the MIT is approached from the metallic side, but  $S$  itself remains constant at the MIT. For (b), we show that the temperature-dependent

$\sigma$ , the thermoelectric power  $S$ , the thermal conductivity  $K$  and the Lorenz number  $L_0$  obey scaling as shown in Fig. 4.

## 6 Scaling for interacting, disordered systems

The research presented in the last section clearly supports the scaling hypothesis of localization for *non-interacting* electrons. However, real electrons of course interact [128], and their interaction is of relevance for the transport properties of disordered systems [129, 130, 131], especially in 2D and 1D [132] where screening [5] is much less efficient than in 3D. Recently, these theoretical considerations received a lot of renewed attention due to the experimental discovery of the 2D MIT [133, 131].

In order to theoretically study the effects of the interplay between disorder and interactions, in principle one has to solve a problem with an exponentially growing number of states in the Hilbert space with increasing system size. At present, this can be achieved only for a few particles in 1D and very few particles in 2D [134, 135, 136]. However, in 1994 Shepelyansky [137] proposed to simply look at *two* interacting particles (TIP) in a random environment. He showed that two particles in 1D would form pair states even for repulsive interactions such that the TIP pairs would have a larger localization length

$$\lambda_2 \propto U^2 \lambda_1^2, \quad (11)$$

than the two separate single particles (SP) leading to an enhanced possibility of transport through the system [138]. In Eq. (11) the pair energy is  $E = 0$ ,  $U$  represents the onsite interaction strength and  $\lambda_1$  is the SP localization length. Subsequent works have established that an enhancement due to interaction indeed exists, although the details are somewhat different from Eq. (11) [139].

### 6.1 Using decimation to study TIP in random environments

The obvious failure of the TMM approach to the TIP problem in a random potential [140, 141, 142, 143] has led us to search for and apply another well tested method of computing localization lengths for disordered system: the decimation method [144]. We computed the TIP Green function in 1D at selected energies for 26 disorders between 0.5 and 9, 24 system sizes between 51 and 251, as well as 11 interaction strengths  $U = 0, 0.1, \dots, 1$ . For each such set of parameters, we averaged over at least 1000 samples. Furthermore, we constructed FSS curves (see Fig. 5) and from these curves computed scaling parameters which are the infinite-sample-size estimates  $\xi_2(U)$  [145] of the localization lengths. We found [146, 147] that onsite interaction in 1D indeed leads to a TIP localization length which is *larger* than the SP localization length at  $E = 0$ . However, the functional dependence is not simply given by Eq. (11). Our data follow  $\xi_2(U) \sim \xi_2(0)^\beta$  with an exponent  $\beta$  which increases with increasing  $|U|$  at  $E = 0$ . The best fit was obtained when the

enhancement  $\xi_2(U)/\xi_2(0)$  depends on an exponent  $\beta$  which is a function of  $U$  [148]. For values of  $U > 1.5$  we observe that the enhancement decreases again; the position of the maximum depends upon  $W$  reflecting the expected duality between the behavior at small and large  $U$  [149].

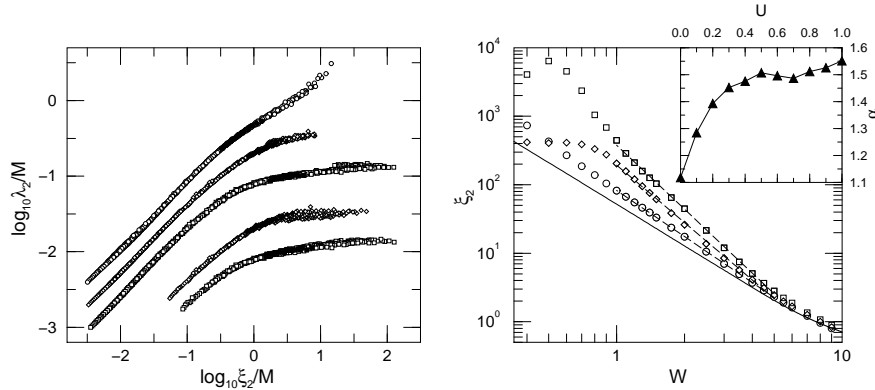


**Fig. 5.** Left: Finite-size scaling plot of the reduced TIP localisation lengths  $\lambda_2/M$  for  $U = 0$  ( $\circ$ ),  $U = 0.2$  ( $\diamond$ ) and  $U = 1$  ( $\square$ ). The data for  $U = 0.2$  ( $U = 1$ ) have been divided by 2 (4) for clarity. Data corresponding to  $W = 1$  are indicated by filled symbols. The two curves at the bottom show the same data for  $U = 0.2$  and 1 and  $W < 2.5$ , shifted downward by one order of magnitude for clarity, but here the data for  $W < 1$  are scaled with scaling parameters obtained from the power-law fits in the right panel. Right: TIP localisation lengths  $\xi_2$  after FSS for  $U = 0$  ( $\circ$ ),  $U = 0.2$  ( $\diamond$ ) and  $U = 1$  ( $\square$ ). The solid line represents 1D TMM data for SP localisation lengths  $\lambda_1/2$ , the dashed lines indicate power-law fits. Inset: Exponent  $\alpha$  obtained by the fit of  $\xi_2 \propto W^{-2\alpha}$  to the data for  $U = 0, 0.1, \dots, 1$ .

## 6.2 The TIP effect in a 2D random environment

In Ref. [150] we have employed the decimation method for TIP in quasi-1D strips of fixed length  $L$  and small cross-section  $M < L$  at  $E = 0$ . Analytical considerations for 2D [138] predict that the enhancement of  $\lambda_2$  at  $E = 0$  should be

$$\lambda_2 \propto \lambda_1 \exp \left[ \frac{U^2 \lambda_1^2}{t^2} \right], \quad (12)$$

with the SP localization length  $\lambda_1 \propto \exp(t^2/W^2)$  in 2D [36]. We found [150] that the enhancement is even stronger and as shown in Fig. 6 the scaling curves for  $U \geq 0.5$  have two branches indicating a transition of TIP states from localized to delocalized behavior [151]. The scaling curves for  $U \leq 0.2$  show a single branch corresponding to localized behavior. The quality of the scaling curves is not as good as in the 1D TIP analysis [146], due to the

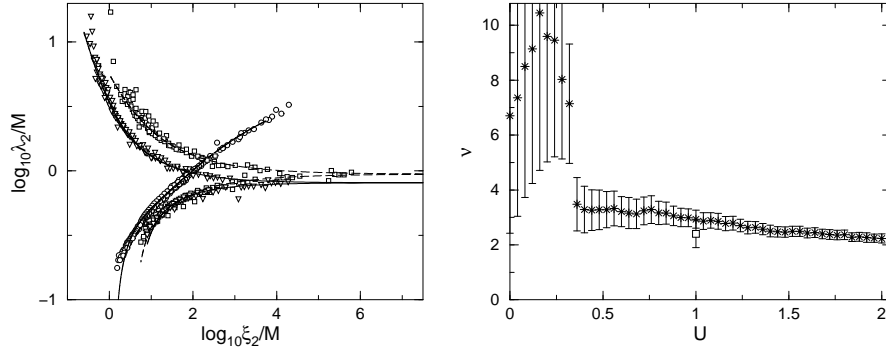


**Fig. 6.** Left: FSS scaling curves (lines) and reduced localization lengths  $\lambda_2/M$  for TIP in 2D as a function of the scaling parameter  $\xi_2$  for  $U = 0$  ( $\circ$ ),  $1$  ( $\square$ ), and  $2$  ( $\nabla$ ). Right: Critical exponent  $\nu$ . The data point ( $\square$ ) for  $U = 1$  represents the result of Ref. [151].

smaller samples and smaller number of configurations. Nevertheless, our data for 51 interaction strengths and 36 disorder values allow us to map the  $(U, W)$  phase diagram of the TIP delocalization-localization transition and we can study how the critical exponent of the localization length changes with  $U$  in Fig. 6. We find that for all  $U \in (0, 2]$ , the exponent is systematically larger than the critical exponent of the usual Anderson transition for non-interacting electrons in 3D. Let us emphasize that this transition is not a metal-insulator transition in the standard sense since only the TIP states show the delocalization transition. The majority of non-paired states remains localized.

### 6.3 The TIP effect close to an MIT

The numerical effort to study the influence of interaction directly at the MIT in 3D is currently prohibitive. This is true even for TIP, since the problem is equivalent to a six-dimensional SP system with correlated disorder. Fortunately, there is a 1D model which exhibits an MIT driven by increasing a local potential. This model is known as the Aubry-André model [152] which we extend by an interaction term, i.e.,

$$H = \sum_{\sigma, n=1}^M (c_{\sigma, n+1}^\dagger c_{\sigma, n} + h.c.) + \sum_{\sigma, n=1}^M \mu_n c_{\sigma, n}^\dagger c_{\sigma, n} + \sum_{n, m=1}^M U_{nm} c_{n\downarrow}^\dagger c_{n\downarrow} c_{m\uparrow}^\dagger c_{m\uparrow}, \quad (13)$$

where  $\mu_n = 2\mu \cos(\alpha n + \beta)$  with  $\alpha/2\pi$  an irrational number chosen as the inverse of the golden mean  $\alpha/2\pi = (\sqrt{5} - 1)/2$ .  $\beta$  is an arbitrary phase shift. The  $c_{\sigma, n}^\dagger$  and  $c_{\sigma, n}$  are the creation and annihilation operators for an electron at site  $n$  with spin  $\sigma = \uparrow, \downarrow$ .  $U_{nm}$  denotes the interaction between particles:  $U_{nm} = U\delta_{nm}$  for Hubbard onsite interaction or  $U_{nm} = U/(|n - m| + 1)$  for

long-range interaction. For  $\mu < 1$ , all SP states in the model with  $U = 0$  have been proven rigorously to be extended, whereas for  $\mu > 1$  all SP states are localized [152, 153, 154, 155, 156, 157, 158]. Directly at  $\mu = \mu_c = 1$  the SP states are critical. Thus the MIT is similar to the MIT in the 3D Anderson model, but there are no mobility edges.

The model has been previously considered at  $U > 0$  from the TIP point of view in Refs. [159, 160, 161]. It has been shown that on the localized side, the TIP effects persists, i.e., the TIP localization length  $\lambda_2 > \lambda_1$ . On the extended side, it was argued that the interaction leads to a localization of the TIP states. In Refs. [162, 163], we have used the TMM and decimation together with FSS to study the problem. We use up to  $M = 377$  sites for the decimation method with at least 1000 samples. Let us emphasize that contrary to the problem with TMM for the TIP situation in finite systems, together with FSS the TMM approach can be used to give meaningful results. However, the computed localization lengths are no longer directly the localization lengths of a TIP pair, but rather measure the influence of the presence of the second particle on the transport properties of the first. In addition to investigating the onsite interacting case, we have also studied long-range interactions in Ref. [162]. We find that whereas onsite interaction does not shift the MIT from  $\mu_c = 1$ , long-range interaction might change the MIT towards smaller values  $\mu_c \approx 0.92$ .

For the quasiperiodic many-body system with nearest-neighbor interaction at finite particle density [164, 165] we have recovered the transition at  $\mu_c = 1$  independent of interaction strength, provided we consider densities like  $\rho = 1/2$  which are incommensurate compared to the wave vector of the quasiperiodic potential — an irrational multiple of  $\pi$ . Thus, the low-density TIP case is comparable to finite but incommensurate densities. On the other hand, for commensurate densities, we find that the system can be completely localized even for  $\mu \ll 1$ , due to a Peierls resonance between the degrees of freedom of the electronic system and the quasiperiodic potential. Whereas for repulsive interactions the ground state remains localized, we find a region of extended states for attractive interaction due to the interplay between interaction and quasiperiodic potential. Thus, the physics of the model at finite densities is dominated by whether the density is commensurate or incommensurate and only in the latter case by interaction effects.

## 7 Conclusions

In the preceding sections, we have presented results of transport studies in disordered systems, ranging from modifications of the standard Anderson model of localization to effects of a two-body interaction. Of paramount importance in these studies was always the highest possible accuracy of the raw data combined with the careful subsequent application of the FSS technique. In fact, it is this scaling method that has allowed numerical studies to move

beyond simple extrapolations and reliably construct estimates of quantities as if one were studying an infinite system. Of course, this statement is only a short and perhaps too short summary of the seminal paper by MacKinnon and Kramer [35], in which the FSS technique was first applied to the localization problem.

## Acknowledgements

We gratefully acknowledge financial support by the DFG via SFB393 and priority research program “Quasikristalle” as well as by the DAAD. This paper is dedicated to Bernhard Kramer on the occasion of his 60th birthday. Both authors are grateful to him for many encouraging discussions and stimulating interactions over many years.

## References

1. P. W. Anderson, *Phys. Rev.* **109**, 1492 (1958).
2. D. Belitz and T. R. Kirkpatrick, *Rev. Mod. Phys.* **66**, 261 (1994).
3. B. Kramer and A. MacKinnon, *Rep. Prog. Phys.* **56**, 1469 (1993).
4. P. A. Lee and T. V. Ramakrishnan, *Rev. Mod. Phys.* **57**, 287 (1985).
5. N. W. Ashcroft and N. D. Mermin, *Solid State Physics* (Saunders College, New York, 1976).
6. E. Abrahams, P. W. Anderson, D. C. Licciardello, and T. V. Ramakrishnan, *Phys. Rev. Lett.* **42**, 673 (1979).
7. F. Wegner, *Z. Phys. B* **44**, 9 (1981).
8. G. A. Thomas, in *Localisation and Interactions in Disordered and Doped Semiconductors*, edited by D. M. Finlayson (SUSSP, Edinburgh, 1986), p. 172.
9. M. A. Paalanen and G. A. Thomas, *Helv. Phys. Acta* **56**, 27 (1983).
10. S. Waffenschmidt, C. Pfeleiderer, and H. v. Löhneysen, *Phys. Rev. Lett.* **83**, 3005 (1999).
11. T. F. Rosenbaum, G. A. Thomas, and M. A. Paalanen, *Phys. Rev. Lett.* **72**, 2121 (1994).
12. H. Stupp *et al.*, *Phys. Rev. Lett.* **71**, 2634 (1993).
13. H. Stupp *et al.*, *Phys. Rev. Lett.* **72**, 2122 (1994).
14. P. Häussler, *Phys. Rep.* **222**, 65 (1992).
15. A. Möbius and C. J. Adkins, *Current Opinion in Solid State and Materials Science* **4**, 303 (1999).
16. U. Thomanschefskey and D. F. Holcomb, *Phys. Rev. B* **45**, 13356 (1988).
17. S. Bogdanovich, M. P. Sarachik, and R. N. Bhatt, *Phys. Rev. Lett.* **82**, 137 (1999).
18. S. Bogdanovich *et al.*, *Phys. Rev. B* **60**, 2286 (1998).
19. K. M. Itoh *et al.*, *Phys. Rev. Lett.* **77**, 4058 (1996).
20. B. Sadow *et al.*, *phys. stat. sol. (b)* **205**, 281 (1998).
21. M. Watanabe, Y. Ootuka, K. M. Itoh, and E. E. Haller, *Phys. Rev. B* **58**, 9851 (1998).
22. T. Hayashi, Y. Hashimoto, S. Katsumoto, and Y. Iye, *J. Phys. Chem. Solids* **63**, 1315 (2002).

23. P. E. Lindelof, J. Nørregard, and J. Hanberg, *Phys. Scr. T* **14**, 317 (1986).
24. G. Maret, *Phys. Blätter* **48**, 161 (1992).
25. D. S. Wiersma, P. Bartolini, A. Lagendjik, and R. Righini, *Nature* **390**, 671 (1997).
26. P.-E. Wolf and G. Maret, *Phys. Rev. Lett.* **55**, 2696 (1985).
27. M. Barth, U. Kuhl, and H.-J. Stöckmann, *Phys. Rev. Lett.* **82**, 2026 (1999).
28. H.-J. Stöckmann, *Quantum Chaos - An Introduction* (Cambridge University Press, New York, 1999).
29. S. I. Bozhevolnyi, *Ann. Phys. (Leipzig)* **8**, 717 (1999).
30. B. Bulka, B. Kramer, and A. MacKinnon, *Z. Phys. B* **60**, 13 (1985).
31. B. Bulka, M. Schreiber, and B. Kramer, *Z. Phys. B* **66**, 21 (1987).
32. B. Kramer and M. Schreiber, in *Fluctuations and Stochastic Phenomena in Condensed Matter*, edited by L. Garrido, *Lecture Notes in Physics* (Springer, Berlin, Heidelberg) **268**, 351 (1987).
33. B. Kramer and M. Schreiber, in *Localization in Disordered Systems*, edited by W. Weller and P. Ziesche, *Teubner Texte zur Physik* (BSB Teubner, Leipzig) **16**, 96 (1988).
34. M. Schreiber, B. Bulka, and B. Kramer, in *Proc. 18th Int. Conf. Physics of Semiconductors*, Stockholm 1986, edited by O. Engström (World Scientific, Singapore 1987), pp. 1269-1272.
35. A. MacKinnon and B. Kramer, *Phys. Rev. Lett.* **47**, 1546 (1981).
36. A. MacKinnon and B. Kramer, *Z. Phys. B* **53**, 1 (1983).
37. A. MacKinnon, *J. Phys.: Condens. Matter* **6**, 2511 (1994).
38. K. Slevin and T. Ohtsuki, *Phys. Rev. Lett.* **82**, 382 (1999).
39. B. Kramer and M. Schreiber, in *Computational Physics*, edited by K. H. Hoffmann and M. Schreiber (Springer, Berlin, 1996), pp. 166-188.
40. J.-L. Pichard and G. Sarma, *J. Phys. C* **14**, L127 (1981).
41. M. Schreiber, H. Grussbach, and M. Ottomeier, *Mol. Cryst. Liq. Cryst.* **216**, 67 (1992).
42. M. Schreiber and B. Kramer, in *Proc. 19th Int. Conf. Physics of Semiconductors*, Warschau 1988, edited by W. Zawadzki (Institute of Physics, Polish Academy of Sciences, Warsaw 1988), pp. 87-90.
43. M. Schreiber and K. Maschke, *Phil. Mag. B* **65**, 639 (1992).
44. M. Schreiber and K. Maschke, in *Photonic Band Gaps and Localization*, edited by C.M. Soukoulis, *NATO ARW* (Plenum, New York) B **308**, 439 (1993).
45. M. Schreiber and K. Maschke, in *Quantum Coherence in Mesoscopic Systems*, edited by B. Kramer, *NATO ASI* (Plenum, New York) B **254**, 105 (1991).
46. J. Sak, B. Kramer, *Phys. Rev. B* **24**, 1761 (1981).
47. B. Kramer and M. Schreiber, *J. Non-Cryst. Sol.* **114**, 330 (1989).
48. B. Kramer, A. Kawabata, and M. Schreiber, *Phil. Mag. B* **65**, 595 (1992).
49. V. I. Oseledec, *Trans. Moscow Math. Soc.* **19**, 197 (1968).
50. F. Wegner, in *Localization and Metal-Insulator Transitions*, edited by H. Fritzsche and D. Adler (Plenum, New York, 1985), p. 337.
51. K. Müller, B. Mehlig, F. Milde, and M. Schreiber, *Phys. Rev. Lett.* **78**, 215 (1997).
52. V. Uski, B. Mehlig, R.A. Römer, and M. Schreiber, *Phys. Rev. B* **62**, R7699 (2000).
53. V. Uski, B. Mehlig, and M. Schreiber, *Phys. Rev. B* **63**, 241101 (2001).
54. T. Guhr, A. Müller-Groeling, and H. A. Weidenmüller, *Phys. Rep.* **299**, 189 (1998).

55. F. Haake, *Quantum Signatures of Chaos*, 2nd ed. (Springer, Berlin, 1992).
56. D. J. Thouless, Phys. Rep. **13**, 93 (1974).
57. M. Schreiber and Y. Toyozawa, J. Phys. Soc. Japan **51**, 1537 (1982).
58. M. Schreiber, J. Phys. C **18**, 2493 (1985).
59. M. Schreiber, Phys. Rev. B **31**, 6146 (1985).
60. M. Schreiber, J. Non-Cryst. Sol. **97 & 98**, 221 (1987).
61. M. Schreiber, in *Localisation 1990*, edited by J.T. Chalker, Inst. Phys. Conf. Ser. **108**, 65 (1991).
62. M. Schreiber, in Proc. Int. Conf. *Localization, Interaction and Transport Phenomena in Impure Metals (LITPIM)*, edited by L. Schweitzer and B. Kramer, Suppl. PTB-PG-1 (PTB Braunschweig 1984), pp. 74-77.
63. M. Schreiber and B. Kramer, in *Overview of Cyber 205 Projects in Bochum*, edited by H. Ehlich, K.-H. Schlosser, and B. Wojcieszynski, Bochumer Schriften zur parallelen Datenverarbeitung (Rechenzentrum der Ruhruniversität, Bochum) **11**, 439 (1986).
64. M. Schreiber, Physica A **167**, 188 (1990).
65. H. Aoki, J. Phys. C **16**, L205 (1983).
66. M. Schreiber, in *Computational Physics*, edited by K. H. Hoffmann and M. Schreiber (Springer, Berlin, 1996), pp. 147-165.
67. H. Grussbach, Ph.D. thesis, Johannes Gutenberg-Universität Mainz, 1995.
68. M. Schreiber and H. Grussbach, Phys. Rev. Lett. **67**, 607 (1991).
69. M. Schreiber and H. Grussbach, Phil. Mag. B **65**, 704 (1992).
70. M. Schreiber and H. Grussbach, Mod. Phys. Lett. B **16**, 851 (1992).
71. H. Grussbach and M. Schreiber, J. Lumin. **53**, 137 (1992).
72. M. Schreiber and H. Grussbach, Phys. Rev. Lett. **68**, 2857 (1992).
73. M. Schreiber, in *New Horizons in Low-Dimensional Electron Systems*, edited by H. Aoki, M. Tsukuda, M. Schlüter, and F. Levy (Kluwer, Dordrecht 1992), pp. 167-178.
74. H. Grussbach and M. Schreiber, Phys. Rev. B **48**, 6650 (1993).
75. H. Grussbach and M. Schreiber, Phys. Rev. B **51**, 663 (1995).
76. H. Grussbach and M. Schreiber, Chem. Phys. **177**, 733 (1993).
77. M. Schreiber and H. Grussbach, J. of Fractals **1**, 1037 (1993).
78. A. D. Mirlin and Y. V. Fyodorov, J. Phys. A: Math. Gen. **26**, L551 (1993).
79. H. Grussbach and M. Schreiber, Physica A **191**, 394 (1992).
80. F. Milde, PhD thesis, Technische Universität Chemnitz (2000), <http://archiv.tu-chemnitz.de/pub/2000/0060/index.html>.
81. M. Schreiber, B. Kramer, and A. MacKinnon, Physica Scripta **T25**, 67 (1989).
82. E. Hofstetter and M. Schreiber, Europhys. Lett. **21**, 933 (1993).
83. M. Schreiber, in *Large Scale Molecular Systems - Quantum and Stochastic Aspects. Beyond the Simple Molecular Picture*, edited by W. Gans, A. Blumen, and A. Amann, NATO ASI (Plenum, New York) B **258**, 385 (1991).
84. M. Schreiber and M. Ottomeier, J. Phys.: Condens. Matter **4**, 1959 (1992).
85. B. Kramer, K. Broderix, A. MacKinnon, and M. Schreiber, Physica A **167**, 163 (1990).
86. M. Schreiber and B. Kramer, in *Anderson Localization*, edited by T. Ando, H. Fukuyama, Proceedings in Physics (Springer, Berlin, Heidelberg) **28**, 92 (1988).
87. E. Hofstetter and M. Schreiber, Phys. Rev. B **49**, 14726 (1994).



88. M. Schreiber and F. Milde, in *Computational Statistical Physics - From Billiards to Monte Carlo*, edited by K.H. Hoffmann and M. Schreiber (Springer, Berlin, Heidelberg 2002), pp. 259-278.
89. T. Rieth and M. Schreiber, *Z. Phys. B* **104**, 99 (1997).
90. T. Rieth and M. Schreiber, in Proc. 5th Int. Conf. *Quasicrystals*, edited by C. Janot and R. Mosseri (World Scientific, Singapore 1995), pp. 514-517.
91. M. Schreiber and H. Grussbach, *Phys. Rev. Lett.* **76**, 1687 (1996).
92. F. Milde, R. A. Römer, and M. Schreiber, *Phys. Rev. B* **55**, 9463 (1997).
93. F. Milde, R. A. Römer, M. Schreiber, and V. Uski, *Eur. Phys. J. B* **15**, 685 (2000).
94. F. Milde, R. A. Römer, and M. Schreiber, *Phys. Rev. B* **61**, 6028 (2000).
95. M. L. Ndawana, R. A. Römer, and M. Schreiber, *Eur. Phys. J. B* **27**, 399 (2002).
96. F. Milde and R. A. Römer, *Ann. Phys. (Leipzig)* **7**, 452 (1998).
97. E. Hofstetter and M. Schreiber, *Phys. Rev. B* **48**, 16979 (1993).
98. E. Hofstetter and M. Schreiber, *Phys. Rev. Lett.* **73**, 3137 (1994).
99. I. K. Zharekeshv and B. Kramer, *Phys. Rev. Lett.* **79**, 717 (1997).
100. D. Braun, G. Montambaux, and M. Pascaud, *Phys. Rev. Lett.* **81**, 1062 (1998).
101. H. Potempa and L. Schweitzer, *J. Phys.: Condens. Matter* **10**, L431 (1998).
102. E. N. Economou and P. D. Antoniou, *Solid State Commun.* **21**, 285 (1977).
103. F. J. Dyson, *Phys. Rev.* **92**, 1331 (1953).
104. R. H. McKenzie, *Phys. Rev. Lett.* **77**, 4804 (1996).
105. A. Eilmès, R. A. Römer, and M. Schreiber, *Eur. Phys. J. B* **1**, 29 (1998).
106. A. Eilmès, R. A. Römer, and M. Schreiber, *phys. stat. sol. (b)* **205**, 229 (1998).
107. A. Eilmès, R.A. Römer, and M. Schreiber, *Physica B* **296**, 46 (2001).
108. F. Wegner, *Z. Phys. B* **35**, 207 (1979).
109. R. Gade and F. Wegner, *Nucl. Phys. B* **360**, 213 (1991).
110. R. Gade, *Nucl. Phys. B* **398**, 499 (1993).
111. M. Fabrizio and C. Castellani, *Nucl. Phys. B* **583**, 524 (2000).
112. A. Eilmès and R. A. Römer, *J. Phys. Soc. Japan* (2002), in press.
113. P. Cain, Diploma thesis, Technische Universität Chemnitz (1998).
114. P. Biswas, P. Cain, R.A. Römer, and M. Schreiber, *phys. stat. sol. (b)* **218**, 205 (2000).
115. G. A. Thomas, *Phil. Mag. B* **52**, 479 (1985).
116. M. Lakner and H. v. Löhneysen, *Phys. Rev. Lett.* **70**, 3475 (1993).
117. C. Lauinger and F. Baumann, *J. Phys.: Condens. Matter* **7**, 1305 (1995).
118. G. Sherwood, M. A. Howson, and G. J. Morgan, *J. Phys.: Condens. Matter* **3**, 9395 (1991).
119. C. Villagonzalo and R. A. Römer, *Ann. Phys. (Leipzig)* **7**, 394 (1998).
120. C. Villagonzalo, R. A. Römer, and M. Schreiber, *Eur. Phys. J. B* **12**, 179 (1999).
121. C. Villagonzalo, R. A. Römer, M. Schreiber, and A. MacKinnon, *Phys. Rev. B* **62**, 16446 (2000).
122. G. V. Chester and A. Thellung, *Proc. Phys. Soc.* **77**, 1005 (1961).
123. D. A. Greenwood, *Proc. Phys. Soc.* **71**, 585 (1958).
124. R. Kubo, *J. Phys. Soc. Japan* **12**, 570 (1957).
125. C. Castellani, C. D. Castro, M. Grilli, and G. Strinati, *Phys. Rev. B* **37**, 6663 (1988).
126. U. Sivan and Y. Imry, *Phys. Rev. B* **33**, 551 (1986).

127. J. E. Enderby and A. C. Barnes, Phys. Rev. B **49**, 5062 (1994).
128. C. A. d. Coulomb, French physicist; discoverer and eponym of Coulomb's law, 1736-1806.
129. A. L. Efros and B. Shklovskii, J. Phys. C **8**, L49 (1975).
130. N. F. Mott, *Metal-Insulator Transitions* (Taylor & Francis, London, 1990).
131. M. P. Sarachik and S. V. Kravchenko, Proc. Natl. Acad. Sci. USA **96**, 5900 (1999).
132. T. Giamarchi and B. S. Shastry, Phys. Rev. B **51**, 10915 (1995).
133. S. V. Kravchenko *et al.*, Phys. Rev. B **50**, 8039 (1994).
134. P. H. Song and D. L. Shepelyansky, Phys. Rev. B **61**, 15546 (2000).
135. T. Vojta, F. Epperlein, and M. Schreiber, Phys. Rev. Lett. **81**, 4212 (1998).
136. F. Epperlein, M. Schreiber, and T. Vojta, phys. stat. sol. **205**, 233 (1998).
137. D. L. Shepelyansky, Phys. Rev. Lett. **73**, 2607 (1994).
138. Y. Imry, Europhys. Lett. **30**, 405 (1995).
139. R. A. Römer, M. Schreiber, and T. Vojta, Physica E **9**, 397 (2001).
140. K. Frahm, A. Müller-Groeling, J. L. Pichard, and D. Weinmann, Europhys. Lett. **31**, 169 (1995).
141. R. A. Römer and M. Schreiber, Phys. Rev. Lett. **78**, 515 (1997).
142. K. Frahm, A. Müller-Groeling, J.-L. Pichard, and D. Weinmann, Phys. Rev. Lett. **78**, 4889 (1997).
143. R. A. Römer and M. Schreiber, Phys. Rev. Lett. **78**, 4890 (1997).
144. C. J. Lambert and D. Weaire, phys. stat. sol. (b) **101**, 591 (1980).
145. P. H. Song and D. Kim, Phys. Rev. B **56**, 12217 (1997).
146. M. Leadbeater, R. A. Römer, and M. Schreiber, Eur. Phys. J. B **8**, 643 (1999).
147. R. A. Römer, M. Leadbeater, and M. Schreiber, Physica A **266**, 481 (1999).
148. I. V. Ponomarev and P. G. Silvestrov, Phys. Rev. B **56**, 3742 (1997).
149. X. Waintal, D. Weinmann, and J.-L. Pichard, Eur. Phys. J. B **7**, 451 (1999).
150. R. A. Römer, M. Leadbeater, and M. Schreiber, Ann. Phys. (Leipzig) **8**, 675 (1999).
151. M. Ortuño and E. Cuevas, Europhys. Lett. **46**, 224 (1999).
152. S. Aubry and G. André, Ann. Israel Phys. Soc. **3**, 133 (1980).
153. M. Kohmoto, Phys. Rev. Lett. **51**, 1198 (1983).
154. M. Kohmoto, L. P. Kadanoff, and C. Tang, Phys. Rev. Lett. **50**, 1870 (1983).
155. S. Östlund *et al.*, Phys. Rev. Lett. **50**, 1873 (1983).
156. S. Östlund and R. Pandit, Phys. Rev. B **29**, 1394 (1984).
157. S. D. Sarma, S. He, and X. C. Xie, Phys. Rev. B **41**, 5544 (1990).
158. I. Varga, J. Pipek, and B. Vasvári, Phys. Rev. B **46**, 4978 (1992).
159. A. Borelli, J. Bellisard, P. Jacquod, and D. L. Shepelyansky, Phys. Rev. Lett. **77**, 4752 (1996).
160. A. Borelli, J. Bellisard, P. Jacquod, and D. L. Shepelyansky, Phys. Rev. B **55**, 9524 (1997).
161. D. L. Shepelyansky, Phys. Rev. B **54**, 14896 (1996).
162. A. Eilmes, U. Grimm, R. A. Römer, and M. Schreiber, Eur. Phys. J. B **8**, 547 (1999).
163. A. Eilmes, R. A. Römer, and M. Schreiber, Eur. Phys. J. B **23**, 229 (2001).
164. C. Schuster, R. A. Römer, and M. Schreiber, Phys. Rev. B **65**, 115114 (2002).
165. C. Schuster, R. A. Römer, and M. Schreiber, J. Phys. Soc. Japan (to appear).